



HAL
open science

Experimental identification and rheological modeling of the Mullins effect for carbon black-filled rubber

Grégory Chagnon, Erwan Verron, Laurent Gornet, Gilles Marckmann, Pierre Charrier, Patrice Fort

► **To cite this version:**

Grégory Chagnon, Erwan Verron, Laurent Gornet, Gilles Marckmann, Pierre Charrier, et al.. Experimental identification and rheological modeling of the Mullins effect for carbon black-filled rubber. 8th International Seminar on Elastomers, 2001, Le Mans, France. hal-01008192

HAL Id: hal-01008192

<https://hal.science/hal-01008192>

Submitted on 18 Mar 2018

HAL is a multi-disciplinary open access archive for the deposit and dissemination of scientific research documents, whether they are published or not. The documents may come from teaching and research institutions in France or abroad, or from public or private research centers.

L'archive ouverte pluridisciplinaire **HAL**, est destinée au dépôt et à la diffusion de documents scientifiques de niveau recherche, publiés ou non, émanant des établissements d'enseignement et de recherche français ou étrangers, des laboratoires publics ou privés.



Distributed under a Creative Commons Attribution 4.0 International License

EXPERIMENTAL IDENTIFICATION AND RHEOLOGICAL MODELING OF THE MULLINS EFFECT FOR CARBON BLACK-FILLED RUBBER

GREGORY CHAGNON¹, ERWAN VERRON¹, LAURENT GORNET¹,
GILLES MARCKMANN¹, PIERRE CHARRIER² AND PATRICE FORT²

¹Laboratoire de Mécanique et Matériaux – Division Calcul des Structures
Ecole Centrale de Nantes
BP 92101
44072 Nantes cedex 03, France

²Groupe Trelleborg, Société Modyn
Service Recherche et Innovations
Zone Industrielle Nantes Carquefou
BP 419
44474 Carquefou cedex, France

ABSTRACT

Elastomers exhibit a reduction of stiffness after a first loading cycle during fatigue tests. This phenomenon so-called the Mullins effect is considered as a damage phenomenon which only depends on the maximum stretch. The aim of our work is to identify this damage experimentally. Viscous effects are neglected and the Ogden's strain energy function is adopted. The damage evolution is measured with cyclic experiments of various amplitudes and identified as a decreasing exponential function of the maximum stretch. Finally we demonstrate that experimental data verify the Miehe's model.

KEYWORDS: ELASTOMER, HYPERELASTICITY, DAMAGE, MULLINS EFFECT, EXPERIMENTAL

INTRODUCTION

It is well-known that elastomers exhibit a reduction of stiffness after the first loading cycle of a fatigue experiment. This phenomenon was studied in details by Mullins [1] and is widely known as the *Mullins effect*. Authors propose different approaches to include this phenomenon in constitutive equations: see Bueche [2], Simo [3] or Miehe [4], for example. Particularly, Miehe uses the classical theory of damage mechanics [5] and separates the damage function in two terms. The first term is discontinuous and only depends on the maximum stretch reached during the strain history. The second term stands for the cumulating damage, which is a function of the arc-length of the loading curves. It can be shown experimentally that the discontinuous part of the damage function is sufficient to describe the material damage because 80% of the Mullins effect take place during the first loading cycle.

The present paper deals with the experimental determination of the discontinuous damage function for a natural rubber. The constitutive equation is build by simply

associating a classical hyperelastic model with a damage function that only depends on the maximum stretch. Viscous and hysteresis effects are neglected. That is the reason why the study is performed on loading curves and unloading curves are considered similar to loading curves.

EXPERIMENTS

The material studied is a carbon black-filled rubber. Uni-axial cyclic tests are conducted on flat coupon specimens under controlled strain. The specimens were prepared and tested by Trelleborg/Modyn. For different strain levels (from 25% to 250%), specimens were submitted to five loading and unloading cycles at constant strain rate. An example of experimental data is presented in Figure 1.

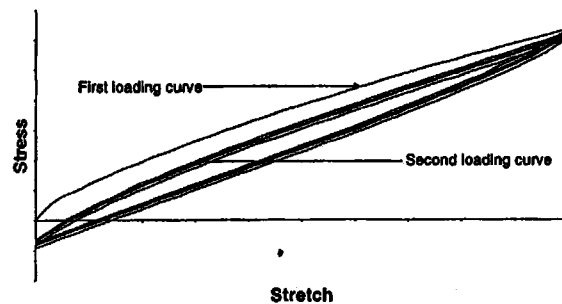


Figure 1. Cyclic loading at a given strain level

As mentioned above, we are only interested in determining the discontinuous part of the damage that takes place during the first loading cycle. Therefore, only the two first cycles are considered. Moreover, hysteresis is removed and only the two first loading curves are studied. These curves are mentioned on the Figure 1.

CONSTITUTIVE MODELING

In the present paper, the Mullins effect is described with a damage function which corrects the strain energy function. The new strain energy function is the product between the damage function $(1-M)$ (or K) and the idealised strain energy, W_0 which corresponds to the undamaged virgin material:

$$W(C, M) = (1-M) \cdot W_0(C) = K \cdot W_0(C) \quad (2)$$

In this equation, M is called the damage parameter and C stands for the right Cauchy Green strain tensor.

Thus, the first Piola-Kirchoff principal stresses are given by:

$$\pi_i = \frac{\partial W}{\partial \lambda_i} \quad i = 1, 3 \quad (3)$$

where λ_i are the principal stretch ratios.

Then:

$$\pi_i = (1-M) \frac{\partial W_0}{\partial \lambda_i} \quad (4)$$

It was observed experimentally that the damage function M only depends on the maximum stretch ratio previously undergone by the material. Consequently, $K=1-M$ is a function of the parameter λ_{max} . This function evolves differently according to the loading curve considered:

- on the first loading curve, λ_{max} is equal to the current value of the uniaxial loading stretch λ and K changes on the curve,

- on the second loading curve λ_{max} is constant (equal to the maximum value attained on the first curve) then K remains constant.

Finally, for every points of the second loading curve, the first Piola-Kirchoff stress tensor is proportional to the corresponding stress tensor of the ideal material defined previously:

$$\pi = K \pi_0 \quad (5)$$

DETERMINATION OF THE DAMAGE FUNCTION

Using reduced experimental data described above, the stress-strain relationship reduces to a sequence of loading curves at different maximum strains. The reduced data are presented in Figure 2.

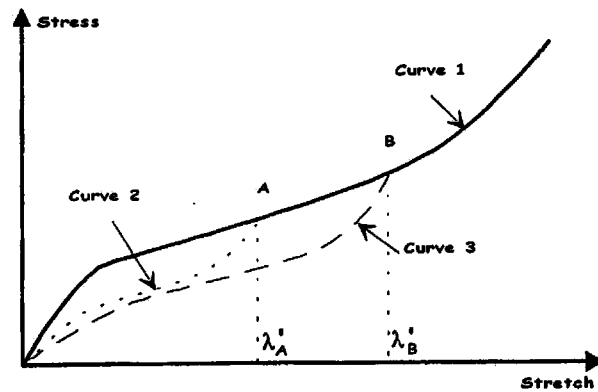


Figure 2. Reduced experimental data.

As mentioned above, the function K evolves according to the loading curve considered:

- on the first curve: K is evolving as loading increases because λ_{max} is growing along the curve : $K = K(\lambda)$

- on the second curve: K is constant

$$K = K(\lambda_{max}) = K(\lambda'_A) \text{ as } \lambda_{max} = \lambda'_A$$

- on the third curve: K is constant

$$K = K(\lambda_{max}) = K(\lambda'_B) \text{ as } \lambda_{max} = \lambda'_B$$

Denoting π_1, π_2, π_3 the stresses on first, second and third curves, respectively, we obtain the following relations :

$$\pi_1(\lambda) = K(\lambda) \pi_0(\lambda) \quad (6)$$

$$\pi_2(\lambda) = K(\lambda'_A) \pi_0(\lambda) = K_2 \pi_0(\lambda) \quad (7)$$

$$\pi_3(\lambda) = K(\lambda'_B) \pi_0(\lambda) = K_3 \pi_0(\lambda) \quad (8)$$

As coefficients K_i are constant for i greater than 1, second loading curves corresponding to different maximum strain values are proportional. Through the end of the paper, notations given in Table 1 are used.

Second loading curve at	Coefficient K
$(i-1) \cdot 25\%$ i from 2 to 11	K_i

Table 1. Proportionality factors between the second loading curves and the first loading curve.

As mentioned above, the undamaged ideal material, i.e. its strain energy function W_0 and the corresponding stresses π_0 , will remain unknown and the determination of K_i can not be performed directly. Therefore, coefficients K_i and K_j are linked together by the ratio of stresses on the second loading curves, π_i and π_j :

$$\frac{K_i}{K_j} = \frac{\pi_i / \pi_0}{\pi_j / \pi_0} = \frac{\pi_i}{\pi_j} \quad (9)$$

Recalling that our model is based on the hypothesis of constant K_i on every loading curve i , we plot the evolution of the ratio K_i/K_{i+1} for every i . An example of such curves is shown in Figure 3.

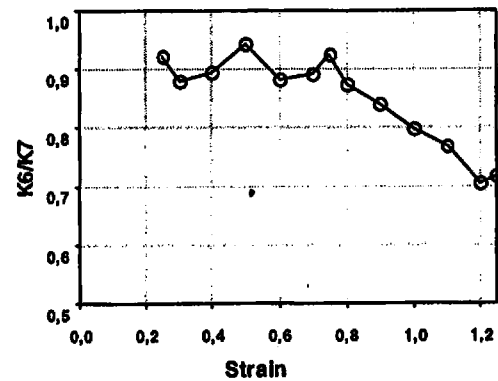


Figure 3. Evolution of the ratio K_6/K_7 versus strain.

These curves present two different parts: for small strains the ratio is constant and for large strains it decreases. This second part of the curve can be related to the strain hardening phenomenon well-known in rubber-like materials. The same observations can be made for all ratios K_i/K_{i+1} . Therefore it is possible to identify the coefficient K_i/K_{i+1} on the first part of the previous curves, noting that a damage model which only depends on the maximum strain is not sufficient to predict accurately the end of second loading curves, i.e. the connection between secondary curves and the first curve

After the determination of all ratios, it becomes possible to study the evolution of the K_i/K_2 ratios (K_2 is defined by the first second loading curve denoted curve 2 in figure 2). Figure 4 presents the evolution of this ratio versus the corresponding maximum stretch imposed during experiments.

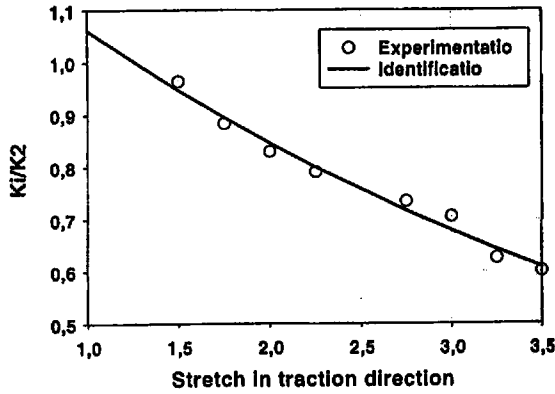


Figure 4. Evolution of K_i/K_2 according to the maximum stretch.

The curve obtained can be identified as a decreasing exponential function:

$$\frac{K}{K_2} = A + B [e^{-\alpha(\lambda_{max}-1)} - 1] \quad (10)$$

Moreover, we must notice that for $\lambda_{max} \rightarrow 0$, the material is unstretched (so, it is not damaged). It is still on the ideal curve and it implies that:

$$A = 1/K_2 \quad (11)$$

Equation (10) becomes :

$$K = 1 + B' [e^{-\alpha(\lambda_{max}-1)} - 1] \quad (12)$$

with

$$B' = B.K_2 \quad (13)$$

Noting $B' = M_\infty$, the discontinuous damage function can be written under the following form:

$$M = M_\infty (1 - e^{-\alpha(\lambda_{max}-1)}) \quad (14)$$

Note that this expression is obtained experimentally and that it coincides with the theoretical form proposed by Miehe [4].

Remark on the limitation of our model : the coefficients that connect the second loading curves being determined, we can superimpose the calculated second loading curve on the same graph. Figure 5 illustrates the superposition of the second loading curves calculated using the proportionality factors K_i and the last second loading curve (at 250%). For small values of the stretch, these curves are superimposed, but they tend to separate each other as the hardening occurs. It illustrates the limitation of the present model, and it confirms the previous remark concerning the form of the curve K_i/K_{i+1} versus λ .

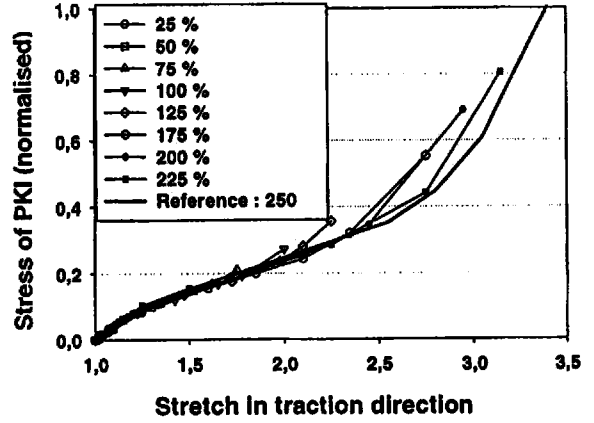


Figure 5. Superposition of the second loading curves.

MODEL IDENTIFICATION

In order to identify the complete constitutive equation, i.e. hyperelasticity and damage, we consider the classical hyperelastic Ogden's model [6]. Moreover, we assume that the rubber remains incompressible.

Here, the three terms version of the model is adopted. The corresponding strain energy function is given by:

$$W = \sum_{n=1}^3 \frac{\mu_n}{\alpha_n} (\lambda_1^{\alpha_n} + \lambda_2^{\alpha_n} + \lambda_3^{\alpha_n} - 3) \quad (15)$$

where λ_i are the principal stretches and $(\mu_n, \alpha_n)_{n=1,3}$ are the material parameters.

For uniaxial extension test, the relation between the first Piola-Kirchoff stress π and the stretch λ in the loading direction is:

$$\pi = \sum_n \mu_n (\lambda^{\alpha_n-1} - \lambda^{-\frac{\alpha_n-1}{2}}) \quad (16)$$

With the damage function this equation becomes:

$$\pi(t) = (1 - \max_{t' < t}(\lambda(t'))) \sum_n \mu_n (\lambda^{\alpha_n-1} - \lambda^{-\frac{\alpha_n-1}{2}}) \quad (17)$$

The parameters of this constitutive equation are identified using experimental data. Results are presented in Figure 6. The results are in good agreement with experimental data except for small strains.

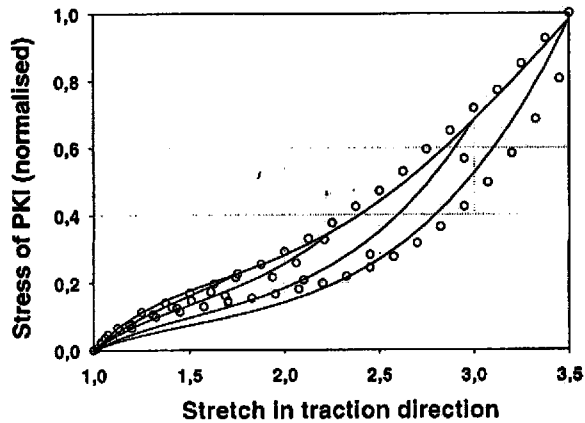


Figure 6. Comparison between theoretical results and experimental data.

CONCLUSION

The present work proposes an experimental method to determine the Mullins effect in natural rubber.

The method is based on the classical theory of damage mechanics.

The damage function obtained by this approach is similar to the theoretical function proposed by Miehe[4]. Moreover using the Ogden strain energy function, the cyclic behaviour of the material is successfully identified. Nevertheless, the important phenomenon of strain hardening observed at the connections between secondary loading curves and the first loading curve is not reproduced by our model. Further work is in progress to take into account the strain-hardening in the damage behaviour.

REFERENCES

1. Mullins, L. 1969 Softening of rubber by deformation, *Rubber Chem. Technol.*, 42, pp. 339-362.
2. Bueche, F. 1960 Molecular basis of the Mullins effect, *J. Appl. Polym. Sci.*, IV, pp. 107-114.
3. Simo, J.C. 1987 On a fully three-dimensional finite-strain viscoelastic damage model: formulation and computational aspects, *Comp. Meth. Appl. Mech. Engng*, 60, pp.153-173.
4. Miehe, C. 1995 Discontinuous and continuous damage evolution in Ogden-type large-strain elastic materials, *Eur. J.Mech. A/Solids*, 14, pp. 697-720.
5. Lemaître, J. et Chaboche, J.L. 1988 *Mécanique des matériaux solides*, Editions Dunod.
6. Ogden, R.W. 1972 Large deformation isotropic elasticity – on the correlation of theory and experiment for incompressible rubberlike solids, *Proc. R. Soc. Lond.*, A326, pp. 565-584.